based on the Euler column formula, using the current steel tangent modulus and an effective unsupported bar length, also user defined. No post-buckling compression models have been implemented for the reinforcement.

Section Stiffness

The section tangent stiffness matrix relates section forces with deformations, following

$$S_s = k_s \; v_s \qquad 13$$

The matrix is determined at each converged state by the standard virtual work integration

$$k_s = \int a_s^T E^t a_s \, dA$$
$$a_s^T = < (y_i - y_o) \; (x_i - x_o) \; -1 > \qquad 14$$

over all fibers (i). In the section and member formulations a trapezoidal integration rule is followed; the actual matrix evaluation is cast into the summations

$$k_s = \begin{bmatrix} \sum_{j=1}^{n} A_j E_j^t y_j^2 & \sum_{j=1}^{n} A_j E_j^t x_j y_j & -\sum_{j=1}^{n} A_j E_j^t y_j \\ \sum_{j=1}^{n} A_j E_j^t x_j y_j & \sum_{j=1}^{n} A_j E_j^t x_j^2 & -\sum_{j=1}^{n} A_j E_j^t x_j \\ -\sum_{j=1}^{n} A_j E_j^t y_j & -\sum_{j=1}^{n} A_j E_j^t x_j & \sum_{j=1}^{n} A_j E_j^t \end{bmatrix} \qquad 15$$

where E_j^t is the current tangent modulus of the j'th fiber evaluated by the material model routines and A_j, x_j, y_j the area and coordinates of the fiber. In the actual implementation, the stiffness terms are evaluated by making use of the fact that different groups of fibers can be defined having equal area. The stiffness is determined about the plastic centroid, the point about which section resisting forces are also reported.

Internal Section Resistances

Calculated strains are fed to the appropriate material model routines in order to establish corresponding stresses. Axial load and bending moments about the two orthonormal axes are estimated by stress integration, again following a trapezoidal rule. Stresses are assumed to be constant within the fiber, equal to the value at the fiber centroid, the location monitored within the program. Following the group program organization, the section load vector is evaluated from the fiber stresses (f_j , of the i'th group) through

$$N = -\left(\sum_{i=1}^{ngc} A_i \sum_{j=1}^{nc} f_{i,j}^{c} + \sum_{i=1}^{ngs} A_i \sum_{j=1}^{ns} f_{i,j}^{s} \right) \tag{16}$$

$$M_x = \sum_{i=1}^{ngc} A_i \sum_{j=1}^{nc} f_{i,j}^{c}\, y_{i,j}^{c} + \sum_{i=1}^{ngs} A_i \sum_{j=1}^{ns} f_{i,j}^{s}\, y_{i,j}^{s} \tag{17}$$

$$M_y = \sum_{i=1}^{ngc} A_i \sum_{j=1}^{nc} f_{i,j}^{c}\, x_{i,j}^{c} + \sum_{i=1}^{ngs} A_i \sum_{j=1}^{ns} f_{i,j}^{s}\, x_{i,j}^{s} \tag{18}$$

where subscripts c and s denote steel and concrete respectively, ngc is the number of concrete groups and ngs the number of steel groups, nc and ns the number of concrete and steel fibers, respectively, per group. Similar double summations are followed in the estimation of the section stiffness previously discussed.

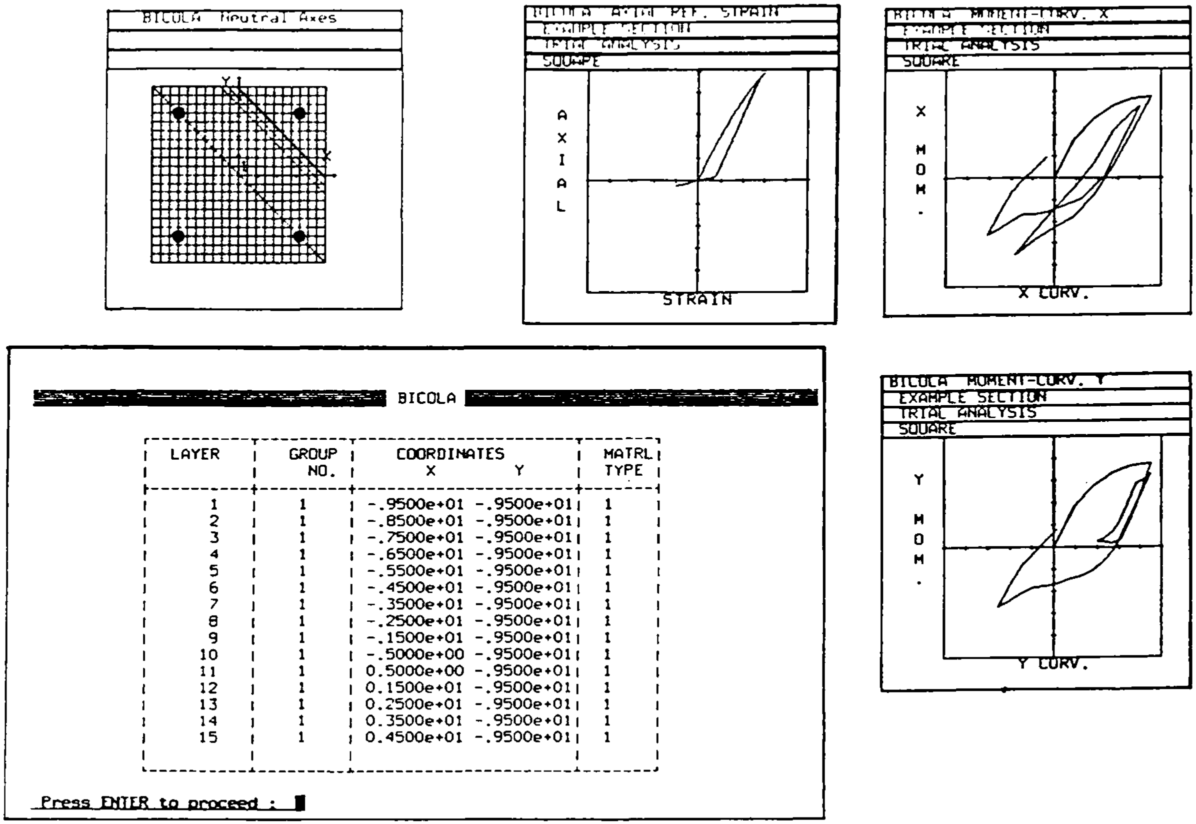

LAYER	GROUP NO.	COORDINATES X	Y	MATRL TYPE
1	1	-.9500e+01	-.9500e+01	1
2	1	-.8500e+01	-.9500e+01	1
3	1	-.7500e+01	-.9500e+01	1
4	1	-.6500e+01	-.9500e+01	1
5	1	-.5500e+01	-.9500e+01	1
6	1	-.4500e+01	-.9500e+01	1
7	1	-.3500e+01	-.9500e+01	1
8	1	-.2500e+01	-.9500e+01	1
9	1	-.1500e+01	-.9500e+01	1
10	1	-.5000e+00	-.9500e+01	1
11	1	0.5000e+00	-.9500e+01	1
12	1	0.1500e+01	-.9500e+01	1
13	1	0.2500e+01	-.9500e+01	1
14	1	0.3500e+01	-.9500e+01	1
15	1	0.4500e+01	-.9500e+01	1

Press ENTER to proceed :

Fig. 1—Typical workstation window while running BICOLA with the GKS graphics

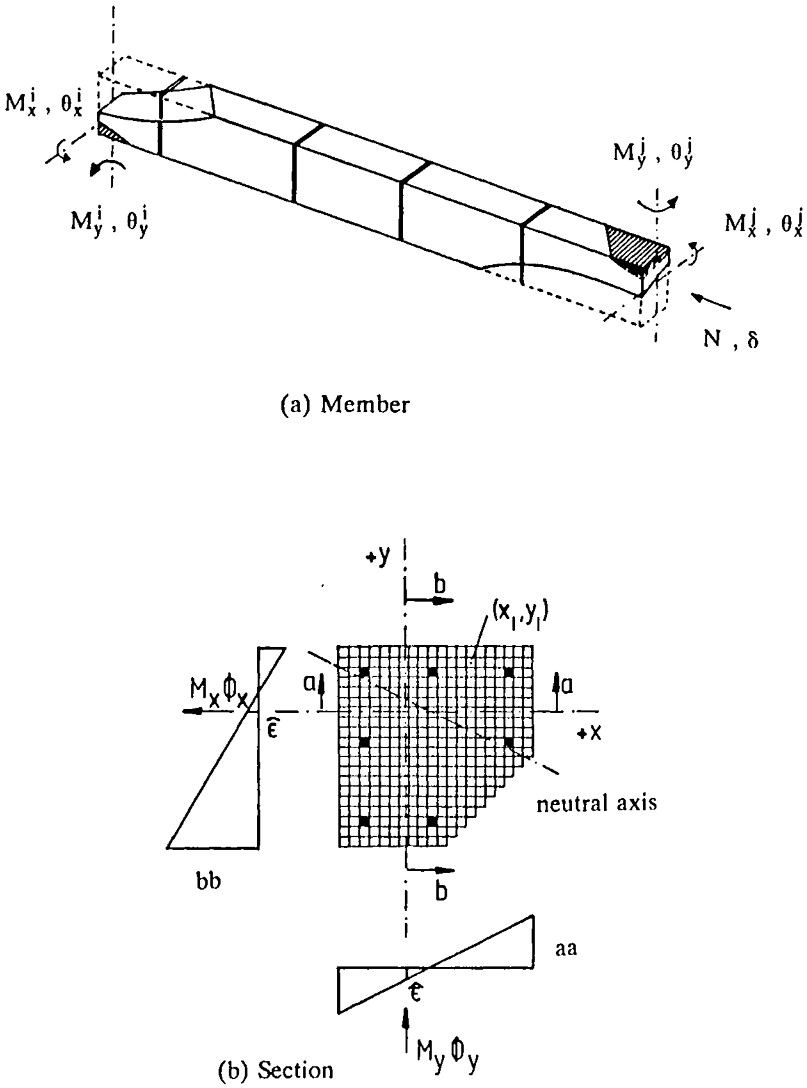

Fig. 2--Member and section idealization

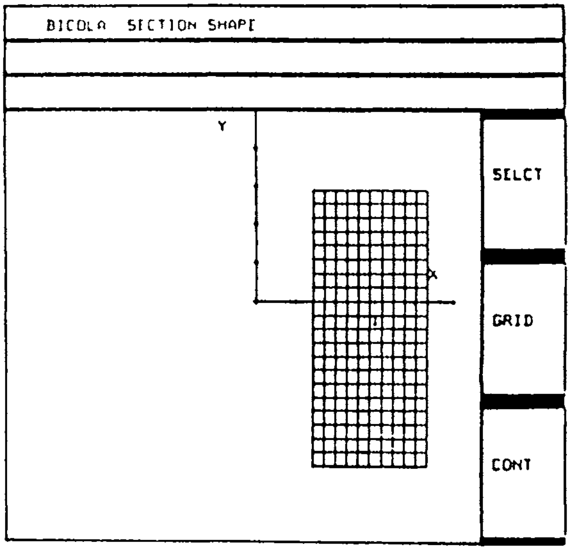

Fig. 3a--Rectangular concrete section primitive

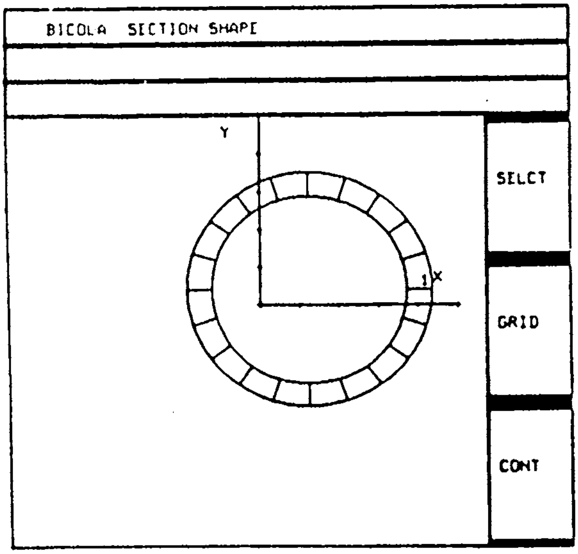

Fig. 3b--Fill concrete section primitive

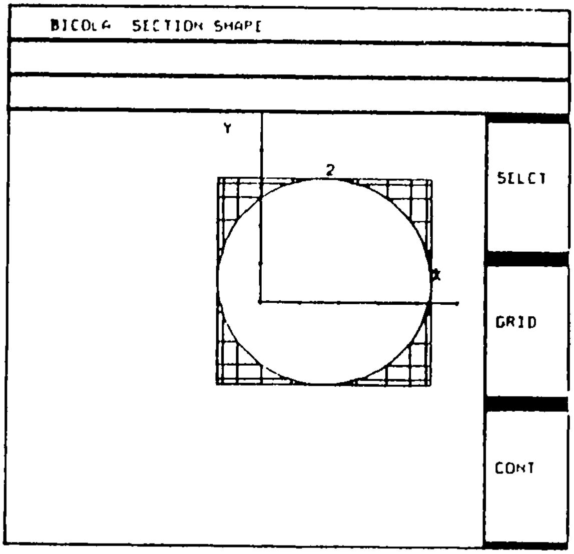

Fig. 3c--Ring concrete section primitive

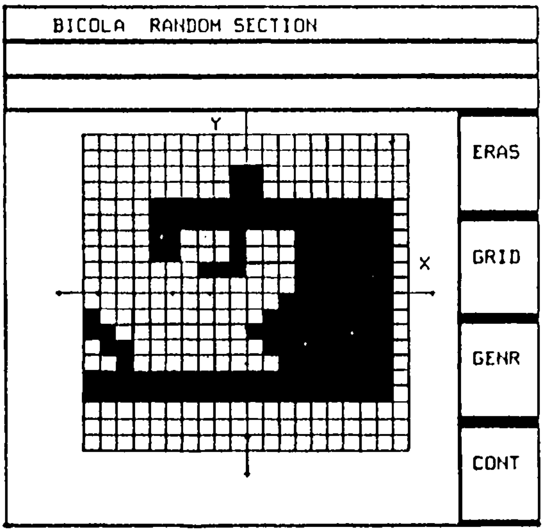

Fig. 3d--Definition of arbitrary shapes on the orthogonal grid

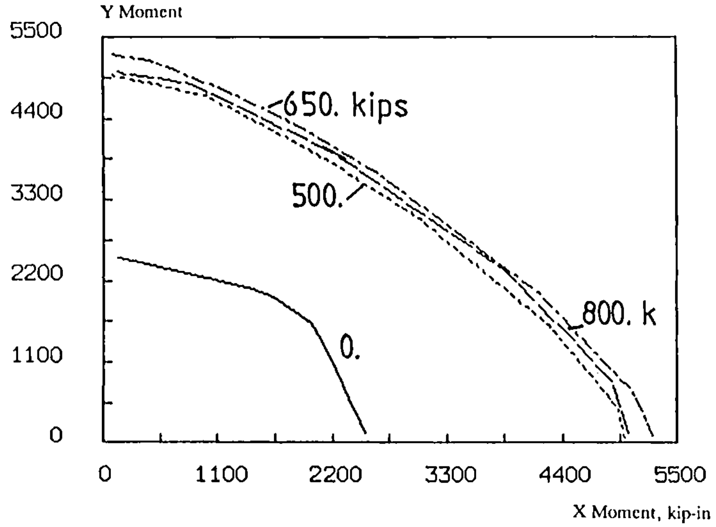

Fig. 4--Biaxial bending interaction diagrams of the example column

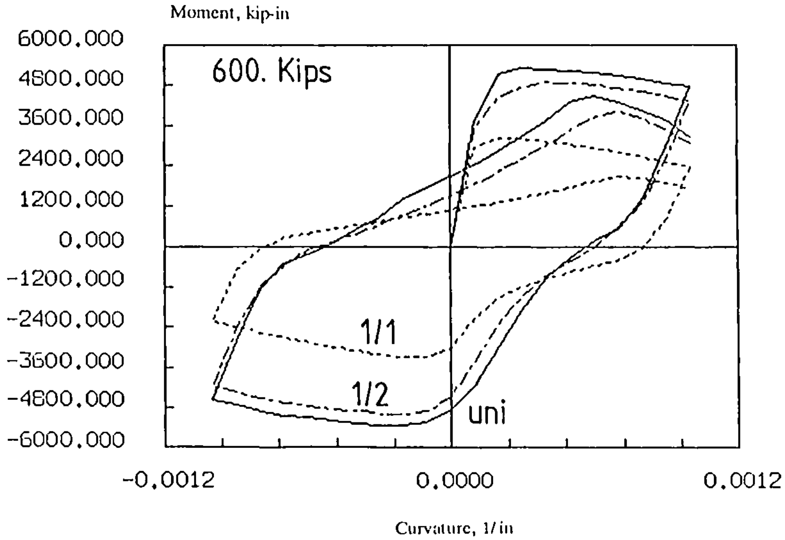

Fig. 5--Biaxial hysteretic response under different curvature ratios

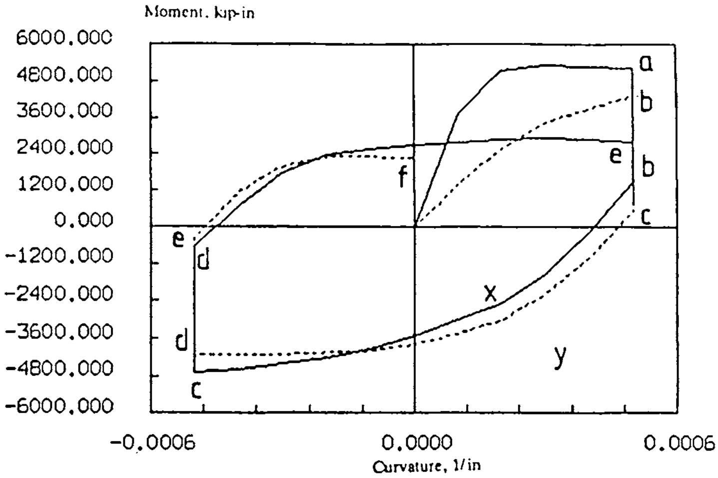

Fig. 6a--Projected hysteretic response

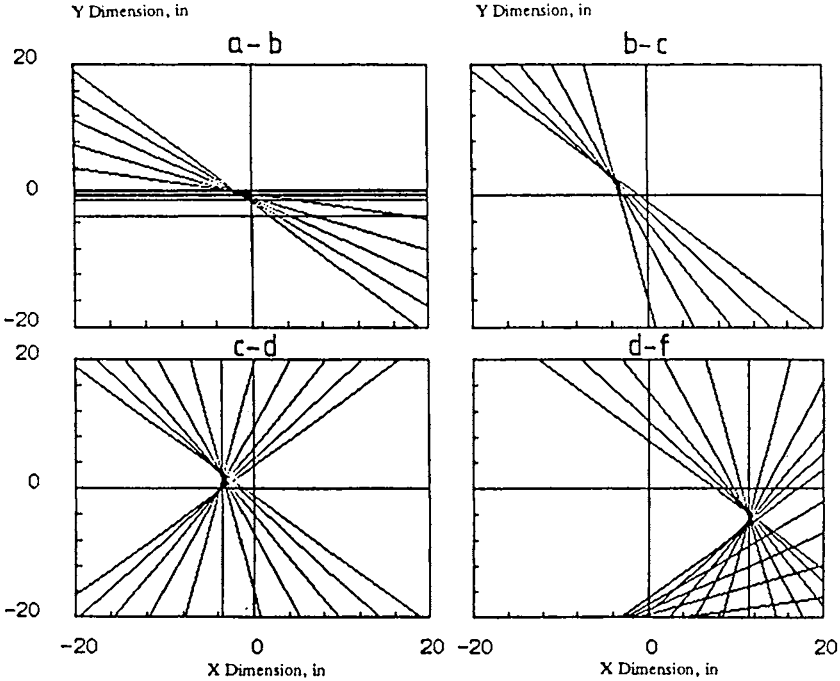

Fig. 6b--Predicted neutral axis movement patterns

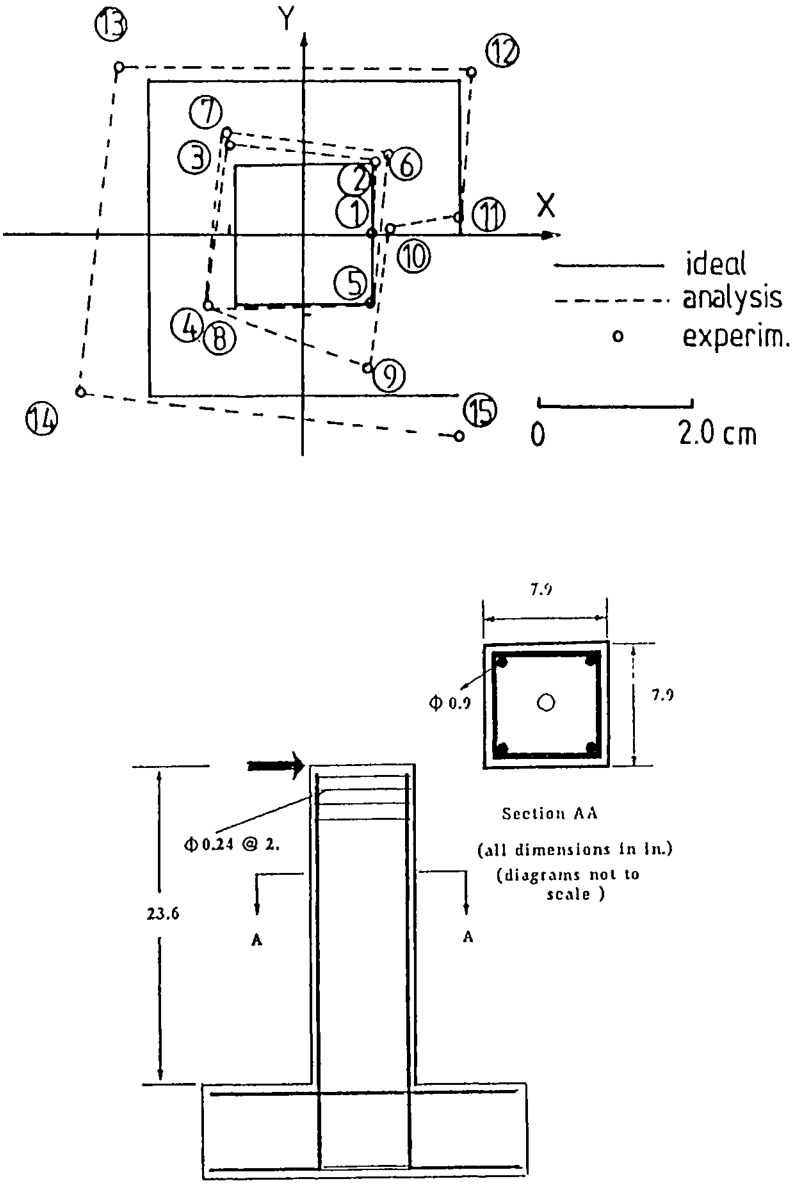

Fig. 7--Specimen detailing and imposed deformation pattern

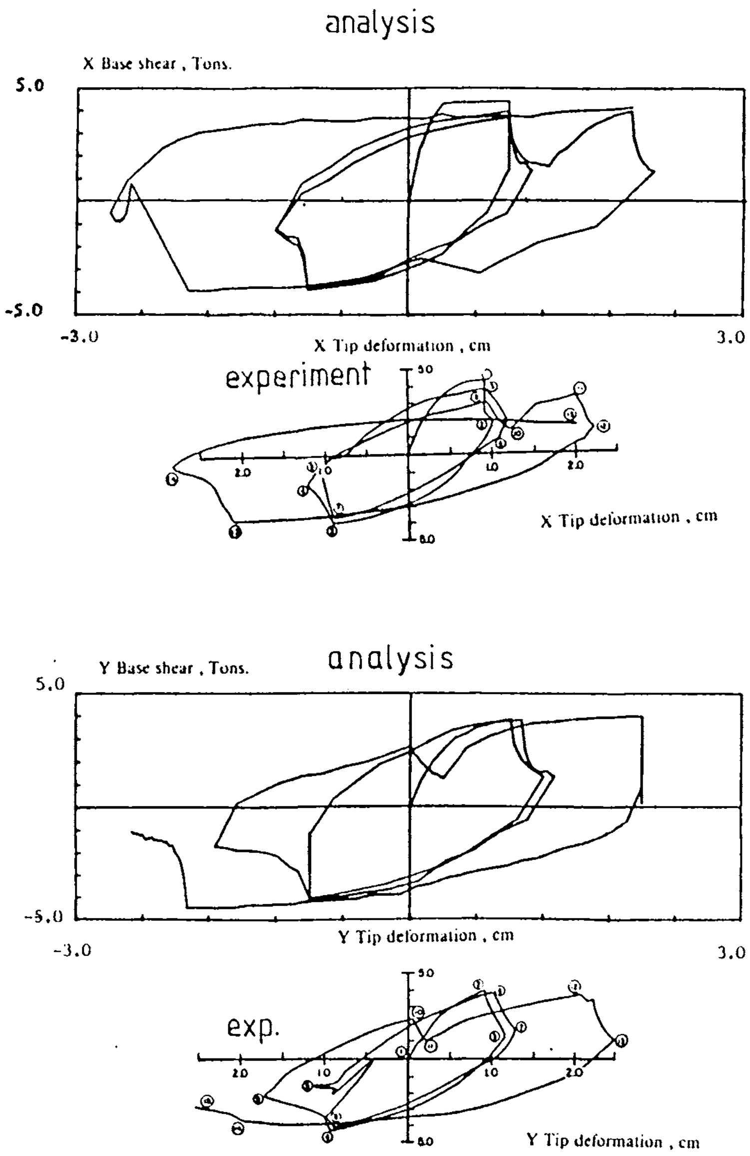

Fig. 8--Comparison of predicted and experimental response